Journal of Applied Fluid Mechanics, Vol. 18, No. 9, pp. 2377-2388, 2025.
Available online at www.jafmonline.net, ISSN 1735-3572, EISSN 1735-3645.
https://doi.org/10.47176/jafm.18.9.3262

Extraction for the Evolution Features of Cavitation Cloud Induced by the Self-excited Oscillating Jet

Z. Hao, K. Li, R. Zhang, Y. Wang and G. Liu†

Institute of Oceanographic Instrumentation, Qilu University of Technology (Shandong Academy of Sciences), Qingdao, Shandong Province, 266100, China

†*Corresponding Author Email: liu-g@qlu.edu.cn*

ABSTRACT

The evolution process of the cavitation cloud in a fluidic oscillator is revealed via the high-speed photography experiment and the extraction of image gray value. The proper orthogonal decomposition (POD) method is employed to extract modal features and analyze the flow fields of a large amount of image data. The basic idea of the POD method is to transform the data into a set of orthogonal basis functions namely eigenmodes or principal components by performing a singular value decomposition of the data matrix. It is found that the first-order mode has a high contribution rate to the flow field, and its shape is nearly identical with the average gray level image of cavitation cloud. Therefore, the first-order mode represents the aggregate average of the gray level field of the cavitation cloud, which means that the large-scale lower order modal structure can reflect the overall stability characteristics of the cavitation cloud. However, the small-scale higher order modal structure reflects the dynamic characteristics such as the development and shedding of the cavitation cloud. With the increase of the inlet flow rate, the stability of the cavitation flow field decreases. By comparing the relationship between the mode coefficient and the average gray value, it is also discovered that the lower order mode coefficient can reflect the variations of cavitation intensity.

Article History

Received November 13, 2024
Revised April 21, 2025
Accepted April 25, 2025
Available online July 5, 2025

Keywords:

Hydrodynamic cavitation
Proper orthogonal decomposition
Fluidic oscillator
Evolution of cavitation cloud
Cavitation intensity

1. INTRODUCTION

Hydrodynamic cavitation is widely applied in various industrial fields. Cavitation occurs when a vapor chamber which could be defined as a region filled with cavitation bubbles forms in the liquid, which is achieved by reducing the local pressure below the saturated vapor pressure (Darandale et al., 2023). Hydrodynamic cavitation can produce a tremendous energy due to the collapse of the cavitation bubbles, which may have adverse effects on mechanical equipment such as material corrosion, noise and vibration. Al-Obaidi (2018) carried out experimental and numerical investigations to explore the cavitation behaviors inside a centrifugal pump. The work of diagnosing cavitation and detecting its level of severity were discussed deeply in the work of Al-Obaidi (2018). Scholars were highly concerned about how to reduce the negative effects of cavitation as demonstrated in the works of Gohil and Saini (2015), Al-Obaidi (2019), Sonawat et al. (2020) and Sun et al. (2022). Nevertheless, with the deepening of related research, it was found that the rational utilization of high-intensity energy released by the collapse of cavitation bubbles could be developed into a type of cavitation jet technology with low energy consumption, wide influence, low cost and no secondary pollution (Simpson & Ranade, 2019; Wang et al., 2021). Recently, cavitation during gasoline or diesel injection has also attracted the scholars' attention as seen in the research of Qiu et al. (2018), Zhang et al. (2023), Wei et al. (2022). The enhanced energy conversion efficiency could be promoted by cavitation in gasoline direct injection according to Zhang et al. (2023). In fact, the cavitation jet, as a new jet technology, is widely used in various modern industrial fields such as sewage treatment, food industry, efficient utilization of energy and biomedicine owing to its characteristics of cleanliness, high efficiency and low cost (Chuah et al., 2015; Song et al., 2022).

With the development of cavitation jet technology and the expansion of application fields, the requirements of jet cavitation performance are becoming increasingly stringent. Therefore, studying the evolution characteristics of cavitation bubbles in during movement and rationally utilizing the energy generated by the collapse of the cavitation bubbles not only has important theoretical value, but also contributes to optimize the design of the cavitation device and develop new types of high-efficiency cavitation device.

In the past decade, some kinds of typical cavitation jet devices such as Venturi tube (Gore et al., 2014; Patil et al., 2014; Pawar et al., 2017) and orifice plate (Dhanke et al., 2018; Dhanke & Wagh, 2020) were employed to generate hydrodynamic cavitation. This is because the internal pressure of the liquid could drop sharply below the saturated vapor pressure (Huang et al., 2013), and scholars have generally investigated the cavitation flow characteristics of these common reactors. Dular et al. (2012) experimentally studied the influence of Venturi test section size on the cavitation structure and dynamics, and explored the influence of structural parameters by scaling the width, height or two dimensions of the section. Long et al. (2017) conducted an experimental study on the cavitation performance of Venturi tubes, exploring the development characteristics of cavity length and the factors affecting cavity growth. Liu et al. (2021a) experimentally investigated the unsteady cavitation flow characteristics under different cavitation numbers, defined the cavitation length based on gray image detection and calculation, and discussed the time characteristics of the cavitation length and the collapse frequency of the cavitation cycle.

Recently, a new type of cavitation reactor, self-excited fluidic oscillator, has drawn significant attention (Hussain & Khan, 2022; Madane & Ranade, 2024). Due to the Coanda effect (Joulaei et al., 2023), the main jet oscillates periodically in the chamber region of the fluidic oscillator under the influence of the feedback loop, resulting in a low-pressure vortex region, and subsequently, a cavitation flow phenomenon is formed. Liu et al. (2022) revealed the characteristics of hydrodynamic cavitation in the jet oscillator through high-speed photography. They studied the development stages of cavitation in each region through the image processing method of extracting gray values, and obtained the relationship between the cavitation number and the cavitation intensity which could be reflected by gray values of the images. It has been demonstrated that fluidic oscillators can also produce intense cavitation phenomena, but further exploration is required. For the fluidic oscillators, scholars are still primarily concerned with the flow characteristics of single-phase fluid inside the oscillator (Seo et al., 2018; Kim & Kim, 2019; Woszidlo et al., 2019; Wu et al., 2019).The evolution features of cavitation cloud induced by the self-excited oscillating jet have not been clearly described, which may limit the enhancement of cavitation intensity.

In the work of Liu et al. (2022), the development characteristics of cavitation clouds including the stages of appearance, development and collapse have been explored through gray value of the high-speed images. It is well known that due to the randomness of cavitation flow, cavitation flow is quasi-periodic rather than truly periodic flow. In fact, another algorithm named Proper Orthogonal Decomposition (POD) is a data analysis method that can decompose large-scale data sets including a series of matrix data (Chatterjee, 2000), which is used to extract the main coherent characteristics of cavitation bubbles and statistical data of cavitation flows. It can decompose the time series of vector or scalar fields into a set of basic spatial patterns and time coefficients thus obtaining the coherent cavitation structure of unsteady cavitation flow. It is commonly used in the field of signal recognition and image processing. The modes and dynamics derived from the POD method represent different characteristics and changes during the cavitation process. By analyzing these modes, the important structure, vortex, oscillation such as in the cavitation phenomenon can be revealed, which helps researchers to understand and explore the mechanism and characteristics of the cavitation phenomenon.

Recently, numerous scholars have also introduced POD into the field of cavitation to analyze turbulence and cavitation flow. The development of the cavitation clouds within a quasi-two-dimensional confined space could be reflected by the methodology of using gray value provided by a camera as noted in the work of Liu et al. (2021a). The POD method was also employed in the work of Xu et al. (2020) to explore cavitation performance in a Venturi reactor. Ge et al. (2022) introduced POD into the field of cavitation for the analysis of turbulence and cavitation flow. The dominant coherent structures of hydrodynamic cavitation were explored using the POD method in the work of Liu et al. (2021b). Danlos et al. (2014) analyzed sheet or cloud cavities as different cavitation states by the POD method. Feng et al. (2011) utilized PIV technology and POD method to analyze the changes of POD energy, mode, coefficient, corresponding main frequency and reconstructed longitudinal vorticity field with various control parameters, indicating that POD modes based on flow direction and vertical velocity exhibit regular changes with different wake vortex shedding states. The POD method could be used to study the ventilation cavitation flow around the bluff body, focusing on the vortex shedding behavior in the wake (Wang et al., 2018). Xu et al. (2022) experimentally used the x-t diagram and POD method to study the flow dynamics and cavitation structure caused by axisymmetrical Venturi segment/cloud cavitation detachment under different flow conditions. They described the coherent structure of sheet cavitation, transition zone and cloud cavitation structure and the characteristics of their changes with displacement and cycle time. Hu et al. (2023) conducted cavitation evolution state experiments in a self-sustained oscillation chamber, analyzed the flow characteristics of shear cavitation in Helmholtz nozzle, and adopted POD method to analyze the cavitation flow structure and detect the shedding mechanism. They clarified the relationship between the cavitation intensity in the nozzle and pulse jet performance under different flow conditions.

From the above, it can be seen that due to the Coanda effect, the main jet can form a cavitation flow phenomenon inside a fluidic oscillator. However, the evolution features of cavitation cloud in the oscillator have not been described clearly, which may limit the improvement of cavitation intensity. The POD method can provide an effective data analysis tool for us to deeply understand the characteristics of the flow field. Nevertheless, few studies have applied POD method to explore the cavitation phenomenon in fluidic oscillators.

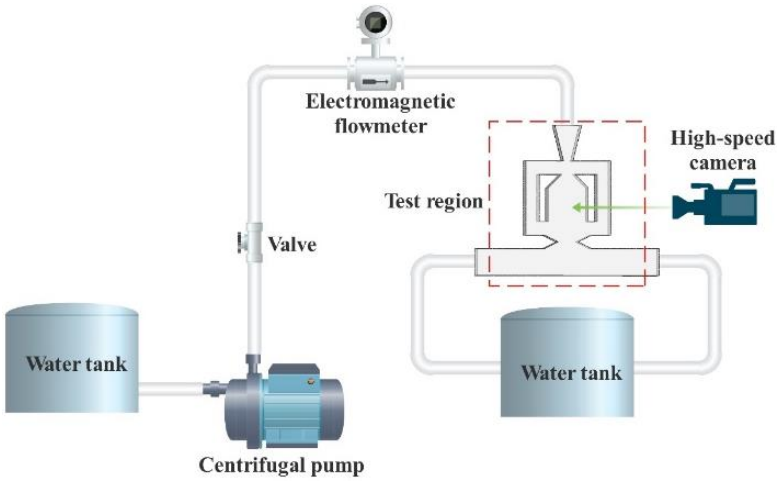

Fig. 1 Experimental system diagram

Therefore, the main objective of this work is to extract the evolution features of cavitation cloud in a fluidic oscillator by the POD method. The results can provide theoretical support for further enhancing cavitation efficiency.

To explore the spatio-temporal distribution characteristics and flow field characteristics of the cavitation cloud inside the fluidic oscillator, this paper employs high-speed camera to obtain cavitation images, extracts gray values to conduct a series of analyses of cavitation intensity, explores the space-time distribution of cavitation in different regions under different flow rates, and deeply comprehends the characteristics and evolution law of cavitation phenomenon. Finally, the modal distribution of the flow field is utilized to extract POD method, and the characteristics of the flow field inside the oscillator are studied.

2. EXPERIMENTAL SETUP

2.1 Experimental Procedure

As shown in Fig. 1, the cavitation jet experimental device mainly consists of a fluidic oscillator, a centrifugal pump, an electromagnetic flowmeter, and a high-speed camera system. The fluidic oscillator is mainly composed of a jet inlet, a nozzle, a feedback loop, a chamber region, and a jet outlet. Since the cavitation process in the fluidic oscillator needs to be directly observed and measured, the main body of the oscillator used in the experiment is made of plexiglass (PMMA, polymethyl methacrylate). The chamber of the oscillator is supplied with water by a centrifugal pump and flow rate is measured by an electromagnetic flowmeter. The measurement range of the electromagnetic flowmeter is 0~2 m^3/h. And the uncertainty of the liquid flow rate is ±1%. To further control the liquid flow, a valve was installed in the experimental loop. In the experiment of any flow rate, the valve remained open throughout.

Before the experiment, the water level in the tank is adjusted to an appropriate level. After completing the preparation work, the regulating valve is adjusted to a suitable opening to obtain the required inlet flow. The data acquisition system is employed to record the flow rate at the cavitation stages including the appearance, development and collapse of cavitation cloud. The cavitation cloud in the oscillator cavity is visually observed at four different inlet flow rates of 0.452 m^3/h, 0.525 m^3/h, 0.575 m^3/h and 0.602 m^3/h.

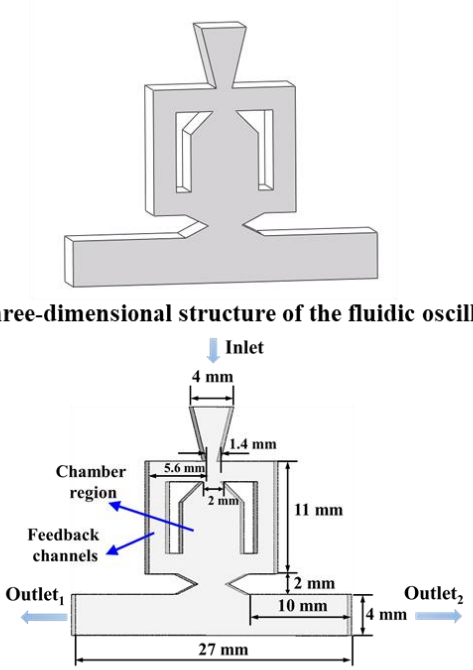

(a) Three-dimensional structure of the fluidic oscillator

(b) Geometric dimensions of the fluidic oscillator

Fig. 2 Fluidic oscillator model diagram

The main structure and some key geometrical parameters of the fluidic oscillator include jet inlet, nozzle, feedback loop, oscillation cavity and jet outlet, as presented in Fig. 2. The oscillator has a thickness of 4 mm. At each cavitation stage, an image needs to be captured, and the cavity of the oscillator, the LED lamp board, the high-speed camera, and the computer together constitute the acquisition system of the cavitation image. In Fig.

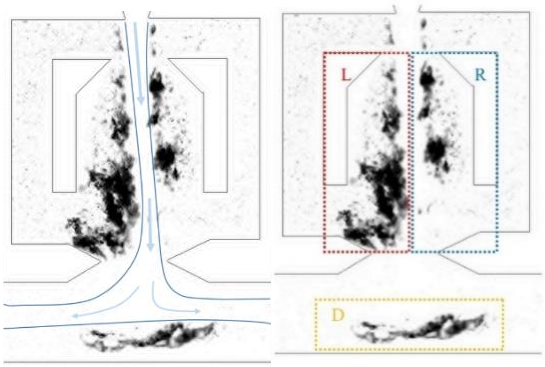

Fig. 3 Cavitation morphology obtained by the high speed camera technology in the fluidic oscillator and three regions including L, R and D in the oscillator

2, the direction of liquid flow and the size of the chamber can be seen. A high - speed camera system recorded the cavitation process. In order to capture the details of cavitation and obtain better shooting effect, a shooting frame was set at 10000 fps. With the flow of the main jet, the cavitation flow field exhibits different characteristics.

The test section is photographed by a high-speed camera system and adopts the backlight method. The backlight becomes evenly dispersed after passing through the scattering plate, which is convenient to adjust the shutter and threshold of the camera during the experimental image observation. In backlight, the light beam is blocked by the gas phase, so the black region represents the cavitation region, and the white region is the liquid phase. The picture of the cavitation cloud taken is presented in Fig. 3(a). In addition to the overall analysis of the cavitation phenomenon, this paper mainly conducts a test analysis on the three regions of L, R, and D in Fig. 3(b).

After the jet is stabilized, the cavitation region of the oscillator is continuously photographed by high-speed photography, and 2000 continuous images recorded are used as the test data under a certain flow rate.

2.2 Image Processing Algorithm

First, the image difference method is used to differentiate the target image and the background image, so as to remove the redundant elements such as the background environment. Subsequently, it is cropped to an appropriate size to highlight the cavitation cloud region to be studied, and then the image is converted into a grayscale image to extract the gray value of the image.

To facilitate image analysis, all the original images are initially converted from RGB images to grayscale. When cavitation occurs, light is reflected at the interface betwween the cavitation bubble and water. Under the same illumination conditions, the brightness of the cavitation region and the non-cavitation region is different. especially in different cavitation regions, due to the difference in the rate of cavitation, the brightness is also different. This technique has been widely applied in the recognition of two-phase flow. Based on the above principles, the corresponding gray values in the image are naturally different, so that different cavitation intensities can be displayed. Consequently, the gray value of the image can more effectively reflect the morphological details of the cavitation flow.

During shooting cavitation cloud image, the entire experiment area is photographed, which will ingests a large amount of irrelevant debris background, causing background noise and polluting the necessary effective information. In order to avoid the possibility of uneven illumination and lens blur, the image difference method was employed to differentiate the target image and the background image, which can remove the background environment and other superfluous places, highlighting the key research area. After a comparative study, this paper adopts the difference algorithm, which is mainly to determine the difference of the corresponding pixel gray value between the image containing the target object and the background image to establish the operation relationship.

The image obtained by the various algorithm is more uniform, and the contrast between the gray value of the pixel of the target objective and the gray value of the background pixel increases. The target object is more prominent, and the quality of the experimental image is greatly improved.

The spatio-temporal distribution map can effectively illustrate the temporal and spatial distribution characteristics of the cavitation cloud, which is of great significance for analyzing cavitation characteristics. When backlight is used, the cavitation bubble block the propagation of light, weakening the gray intensity to a certain extent. In contrast, the liquid phase allows the light transmission, thus enhancing the gray intensity. Therefore, the movement of the interface between the gas phase and the liquid can be observed in the time series, which can well highlight the global characteristics obtained by the cavitation dynamics. It should be noted that the dimensionless processing is carried out on the gray values to obtain the gray intensity according to the method in the work of Liu et al. (2022)

Proper Orthogonal Decomposition (POD) is a mathematical technique grounded in linear algebra. It is used to reduce the dimensionality of high dimensional data and extract its primary features. The fundamental concept of the POD method is to transform the data into a set of orthogonal basis functions called eigenmodes or principal components by performing Singular Value Decomposition (SVD) on the data matrix. These eigenmodes are arranged in descending order of importance, with the previous modes containing the main modes of change and energy of the data. In the field of cavitation, snapshot POD pertains to POD-based snapshot technology. POD is a dimensionality reduction technique employed to process fluid dynamics simulation or experimental data, which can extract the main modes and structures in the flow field. Snapshot POD applies this technology to the analysis and processing of cavitation images. Cavitation images are typically visualizations of hydrodynamic cavitation phenomena captured via high-speed photography or other imaging techniques. By using the snapshot POD method, these image sequences can be processed to extract the main modes and structures in the

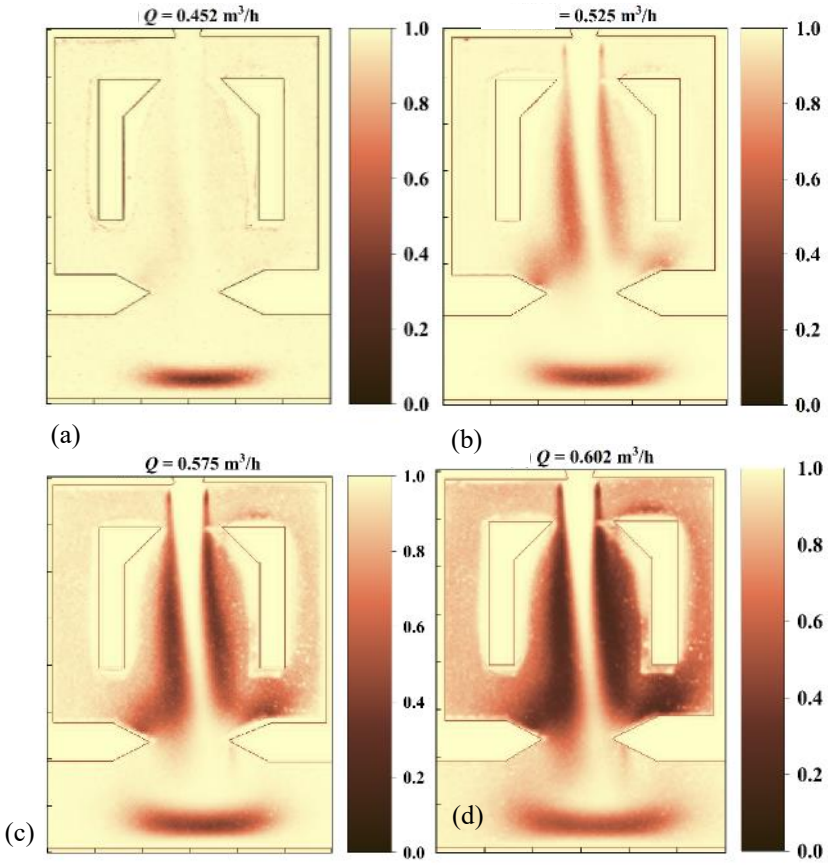

Fig. 4 Average gray level of cavitation cloud under different flow rates

cavitation process for analysis, feature extraction, and understanding. Specifically, snapshot POD decomposes the cavitation image sequence into a set of spatial modes and temporal dynamics through spatiotemporal dimensionality reduction. These modes and dynamics represent diverse characteristics and variations in the cavitation process. By analyzing these modes, we can uncover important information such as structure, vortex, and oscillation in the cavitation phenomenon, assisting researchers in understanding and exploring the mechanism and characteristics of the cavitation phenomenon In this paper, 2000 snapshots of transient cavitation images are selected for POD analysis.

3. RESULTS AND DISCUSSION

3.1 Cavitation Region Analysis

Figure 4 presents the average gray image of the cavitation cloud under the conditions of inlet flow rates, from which the information such as the intensity, shape and location of the development of the cavitation cloud could be obtained. At low flow rate, the cavitation effect in the chamber is less pronounced, and the cavitation is mainly occurring near the mid-region near the exit of both sides of the main jet (Fig. 3, D area). With the increase of flow rate, the cavitation phenomenon becomes more pronounced, and the cavitation cloud formation region gradually expands. A higher flow rate generate stronger vortices and shear forces, promoting the diffusion and growth of the cavitation cloud. This leads to the formation

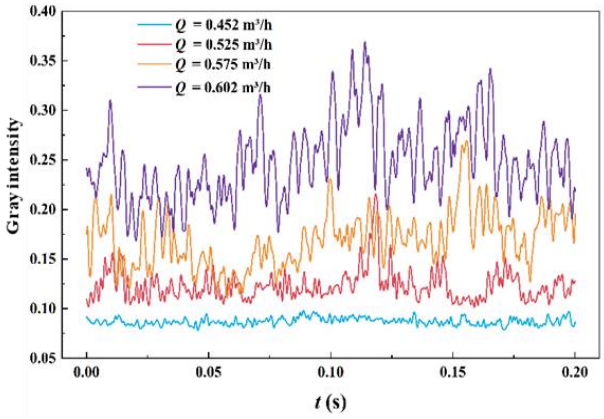

Fig. 5 Temporal distribution of average gray intensity for cavitation cloud under different flow rates

of additional cavitation clouds, which are mainly distributed in the two walls of the main jet and oscillator chamber (Fig. 3, L and R regions). Figure. 5 illustrates the variations of the average gray intensity for each transient cavitation cloud with time under different flow rates, in which the average gray intensity is calculated using normalized gray value. It is evident that with the increase of flow rate, the cavitation intensity gradually increases, the cavitation effect becomes more and more obvious, and the oscillation fluctuation amplitude also increases, which also reflects the instability of cavitation.

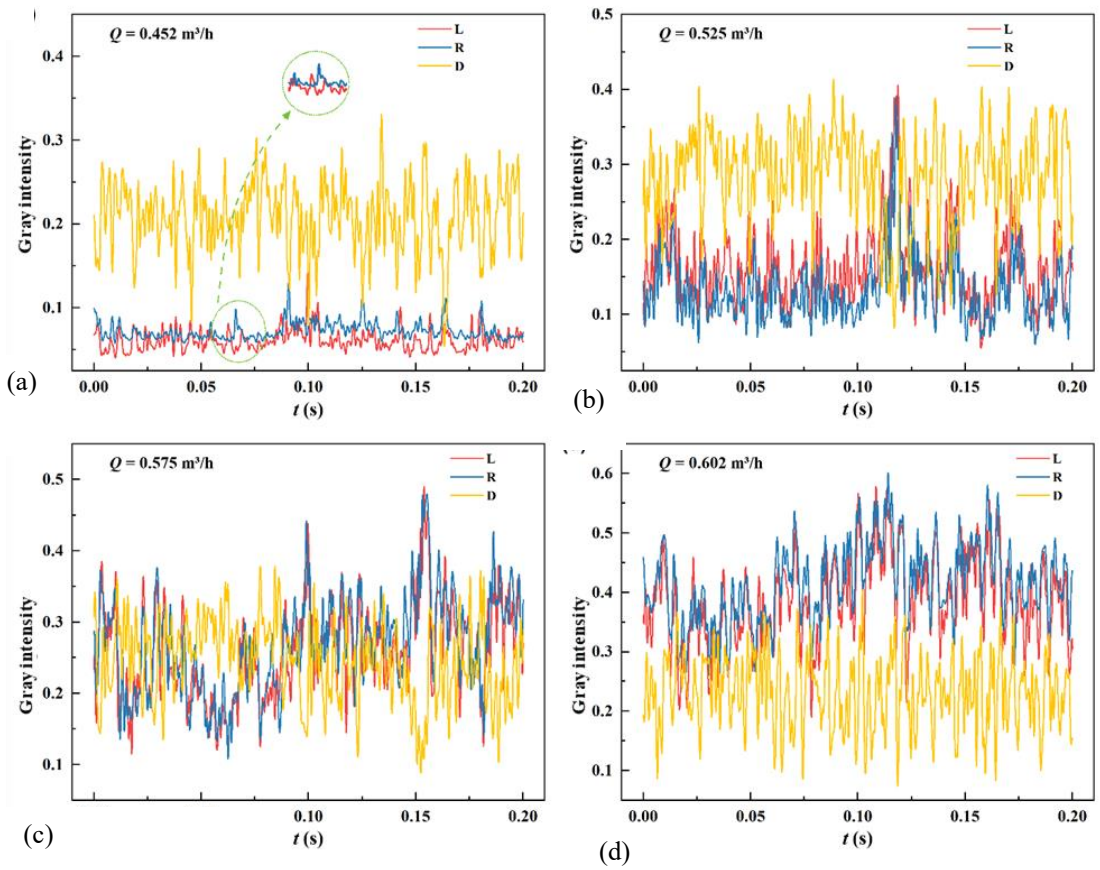

Fig. 6 Time domain variation of average gray intensity of cavitation clouds in three regions

The variation tendency of the average gray intensity of the three regions in Fig. 3 under different inlet flow rates over time is stated in Fig. 6. At low flow rates The cavitation intensity in Region D is stronger, while the cavitation in Region L and Region R is not obvious. However, the cavitation intensities of Region L and Region R are similar and their variation tendencies are similar, and the cavitation evolution on both sides appears alternately, as shown in the part circled by the green dotted line. As the flow rate increases, the cavitation intensities of Region D gradually approach those in Region L and Region R until the inlet flow rate reaches above 0.6 m³/h and finally the cavitation intensities of Region L and Region R become stronger than those of the Region D. Moreover, the gray intensity variation curves of Region L and Region R gradually coincide, indicating that the cavitation intensities of the two regions is almost the same at high flow rates.

3.2 Analysis of Cavitation Flow Characteristics

To illustrate the evolution process of the cavitation cloud more intuitively, Region L is selected to explore the characteristics of cavitation evolution.

Figure 7 shows the evolution process of cavitation cloud in this region over time with the inlet flow rate Q = 0.525 m³/h, and it can be observed that the cavitation cloud exhibits obvious periodic development characteristics. Based on the evolution of the shape of the cavitation cloud, it can be seen that the cavitation is roughly divided into three stages: birth, development and collapse, corresponding to (a)-(b), (c)-(e), and (f)-(j).

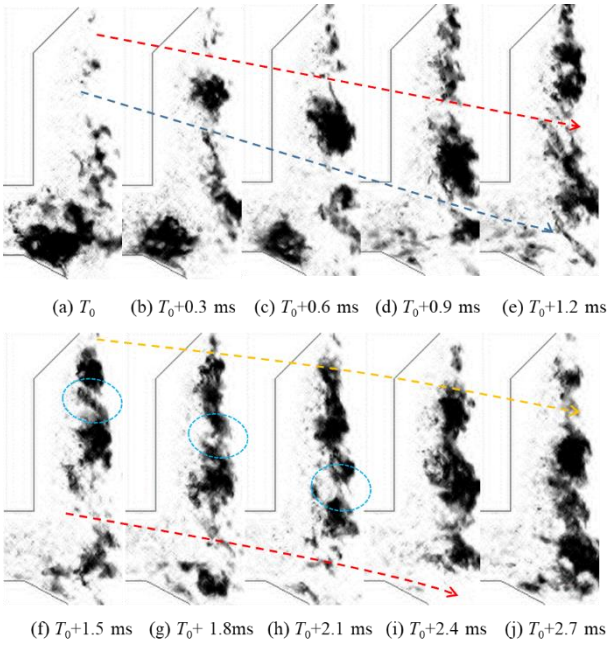

Fig. 7 Evolution of cavitation clouds (Q = 0.525m³/h)

Cavitation occurs when the pressure drops below the saturated vapor pressure. At the initial moment T_0+0 ms, small-scale cavitation bubbles are formed, and gradually converge along the wall at the entrance of the throat to produce a small number of bubbles, while the cavitation cloud of the previous cycle is expanding meanwhile. The

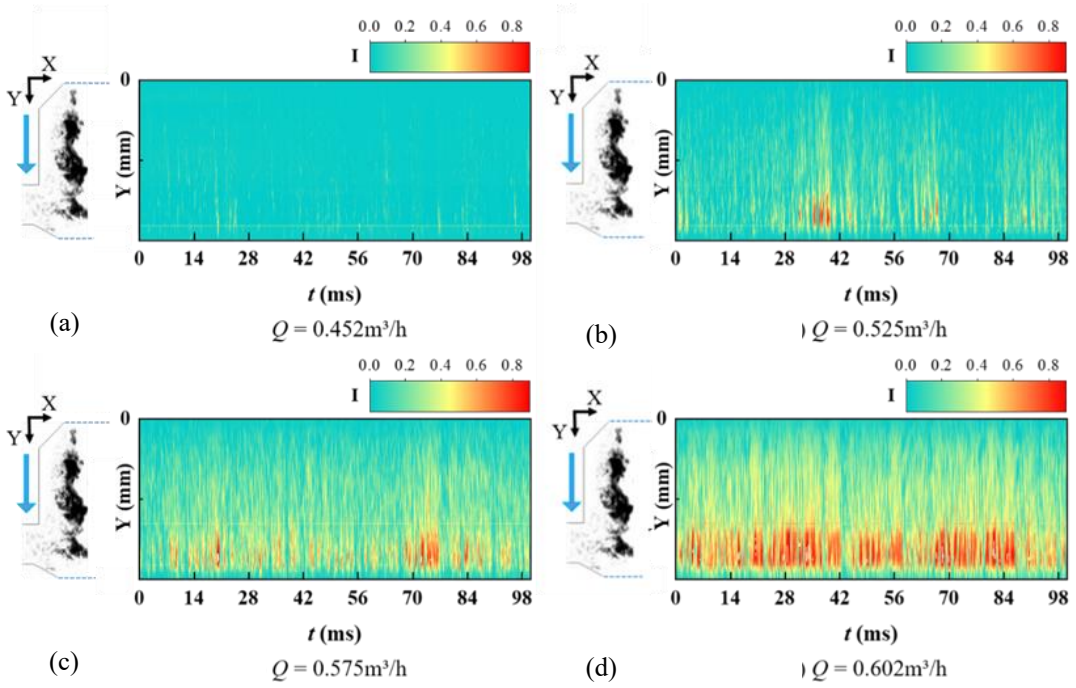

Fig. 8 Space-time distribution of cavitation clouds

dashed blue line in Fig. 7 shows the evolution cavitation evolution in the previous cycle. At the same time, it indicates the beginning of cavitation in the current cycle, and this becomes the initial stage of cavitation. The red dotted line in the corresponding figure shows the evolution process of cavitation in this period. As the flow continues, a large number of small-scale bubbles coalesce and flow downstream along chamber walls. At the moment T_0+0.6 ms, a large number of small cavitation bubbles gradually develop into cavitation clouds. Subsequently, the cavitation cloud expands continuously along the flow direction and becomes larger until the moment T_0+1.2 ms, when the shape of the cavitation cloud reaches its maximum. This stage is termed the development stage of cavitation. As the cavitation cloud continues to develop, its tail gradually becomes unstable. At the moment T_0+1.2 ms, the area circled by the dashed blue line in the figure shows that the middle of the cloud has a tendency to fall off. Its edges gradually begin to crumble into a large number of sparse small bubbles, and the cavitation cloud gradually falls off. This process becomes the collapse stage of cavitation. At the same time, the cavitation cloud of the previous cycle gradually disappeared and collapsed, and the cavitation cloud of the next cycle began to develop, as shown by the yellow dotted line in the figure. Eventually, the cavitation cloud gradually vanishes. In fact, it can be seen from the figure that the evolution period of the cavitation cloud is very short, and one cycle always develops and changes concurrently with the neighboring cycle.

Figure 8 shows the temporal and spatial distribution of the cavitation cloud for the four inlet flows. Y represents the average gray value along the jet flow direction in each transient time study area, and then expands along the time series, which represents the periodic oscillation of the cavitation intensity of the cavitation cloud over time. The different gray values in the space-time map are converted to different colors for better observation. As can be seen from the figure, the motion of the cavitation cloud is decomposed into small typical components containing the periodic behavior of cavitation in different states. By observing the distribution and location of the cavitation phenomenon, it can be seen that the cavitation intensity is weak at the entrance of the oscillator, indicating that the cavitation cloud the incipient emergenc, as the jet moves downstream, the cavitation cloud develops further, and the cavitation intensity is stronger near the exit. However, at low flow rates, the cavitation phenomenon is weak and unevenly distributed. With the increase of flow rate, the cavitation phenomenon gradually becomes obvious, the cavitation cloud is distributed more evenly and densely, and the evolution speed is faster and more sustained. At high flow rates, different cavitation clouds may interact with one another, such as colliding, merging or interfering. These interactions can change the morphology and evolution trajectory of the cavitation cloud, thus affect the overall distribution and morphological characteristics of the cavitation cloud.

The growth, shedding, and collapse process of the cavitation cloud exhibits certain periodicity. Understanding these characteristics is helpful to improve the performance and stability of jet system. The results show that pump pressure, flow rate, nozzle structure and other parameters have significant effects on the evolution period of cavitation cloud. In this paper, the gray mean value of a large amount of image data is extracted by image gray processing method, and the frequency domain analysis is conducted to further reveal the dynamic characteristics of the cavitation cloud. Figure 9 shows the spectrum diagram of the global average gray value for four different inlet flow rates. As can be observed from the

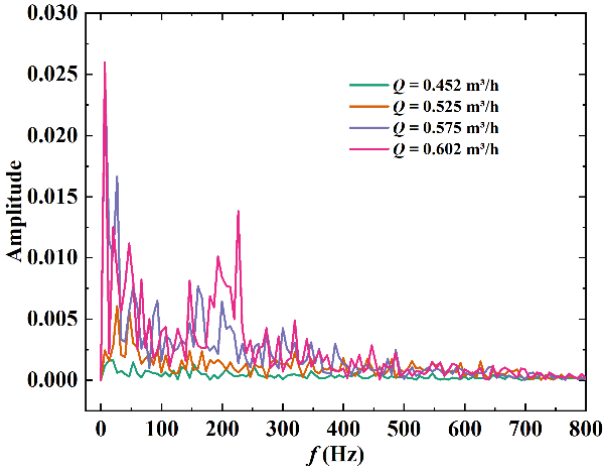

Fig. 9 Spectral diagram of gray intensity at different flow rates

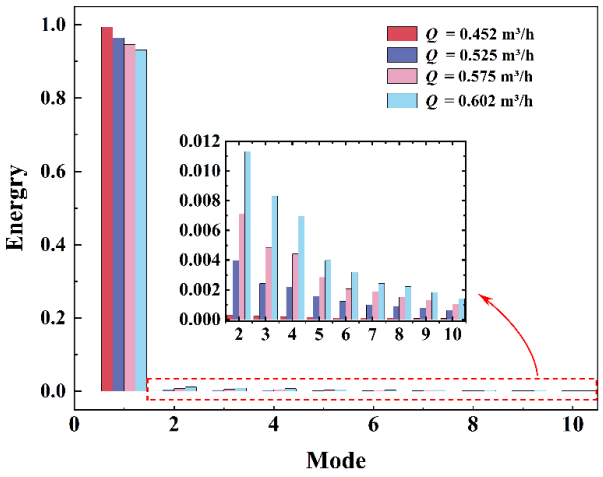

Fig. 10 Top ten POD modes energy contributions

spectrum diagram that the main frequency is not obvious at low flow rate, while the high frequency component gradually increases with the increase of inlet flow rate. Furthermore, the amplitude fluctuation also increased significantly, indicating that the instability of the cavitation cloud inside the oscillator increased with the increase of the inlet flow. In other words, as the inlet flow increases, the cavitation cloud within the fluidic oscillator becomes more and more unstable.

From the amplitude and frequency trends, it can be found that there is a close correlation between the oscillator inlet flow and the cavitation intensity. With the increase of inlet flow, the fluctuation amplitude of cavitation intensity increases. Besides, the growth and shedding cycles of cavitation clouds become more frequent, which further verifies the influence of inlet flow on cavitation flow.

Figure 10 shows the energy contribution of the first 10 modes of POD of the cavitation cloud under different inlet flow rates, among which the energy of the first mode accounts for over more than 90%, and the energy of the second mode drops sharply. The energy of the second and other higher orders accounts for very little. The results indicate that the lower the mode, the greater the contribution to the cavitation structure, and the first-order mode occupies most of the kinetic energy of the whole flow field. This indicates that the entire flow field is regular, the jet energy is stable, and the local pulsation is weak. And it can reflect the average state of the whole flow field and the effective energy of jet erosion. The contribution of each mode varies under different inlet flow rates, indicating the particularity of each cavitation structure. In addition, Fig. 11 shows the contribution of each mode under different inlet flow rates. It can be observed that the energy of the first-order mode decreases with the increase of the flow rate. While, the energy of the higher-order mode increases with the increase of the flow rate for higher order modes, indicating that the downstream field structure of the low-flow rate is more stable.

Figure 12 shows the first four POD mode graphs for different inlet flow conditions. Compared with the average gray level image of cavitation cloud in Fig. 4, it can be seen that the first-order mode has a large contribution rate to the flow field. The shape is almost consistent with the average gray level image of cavitation cloud. Thus, the first-order mode represents the overall average of the gray level field of the cavitation cloud, which can show the average flow distribution. However, the 2-4 order modes contribute little to the cavitation evolution. They mainly capture the fluctuating energy in the cavitation region, represent the transient component, and reflect the smaller pulsation structures in the cavitation evolution, including the occurrence and collapse of cavitation.

From a longitudinal comparison, when the inlet flow rate is relatively low, the morphology diagram after POD mode decomposition is mainly manifested at the bottom of the oscillator, indicating that cavitation mainly occurs in the bottom region of the oscillator at low flow rate, which is consistent with the previous conclusion. The large-scale structure is decomposed into two small-scale structures with the continuous development of the jet, and presents an alternating distribution state first up and down and then left and right.

When the inlet flow rate is high, the cavitation cloud is mainly distributed in the two wall regions of the oscillator chamber. As shown in the second-order modal diagram, the first two modal structures of the last three flow distributions are similar, which indicates that at high flow rate, the large-scale modal structure with higher energy does not change significantly with the increase of the inlet flow rate. The state corresponding to the second-order mode is likely the growth stage of the cavitation cloud. As the jets flow and the development of the cavitation cloud, the jet structure under different inlet flow rates has a great difference from the third-order mode. With the increase of the mode order, the large-scale structures on the left and right sides gradually move downstream and break down into small-scale structures with an alternating distribution of different rotation directions. The medium and small-scale structures of the flow field gradually becomes disordered, and the diversity keeps increasing, indicating the instability of the

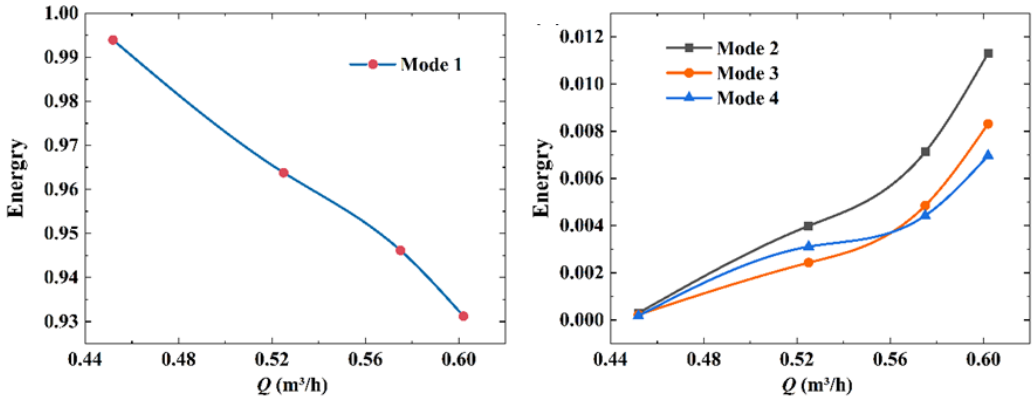

(a) (b)

Fig. 11 Mode contribution of each order under different inlet flows

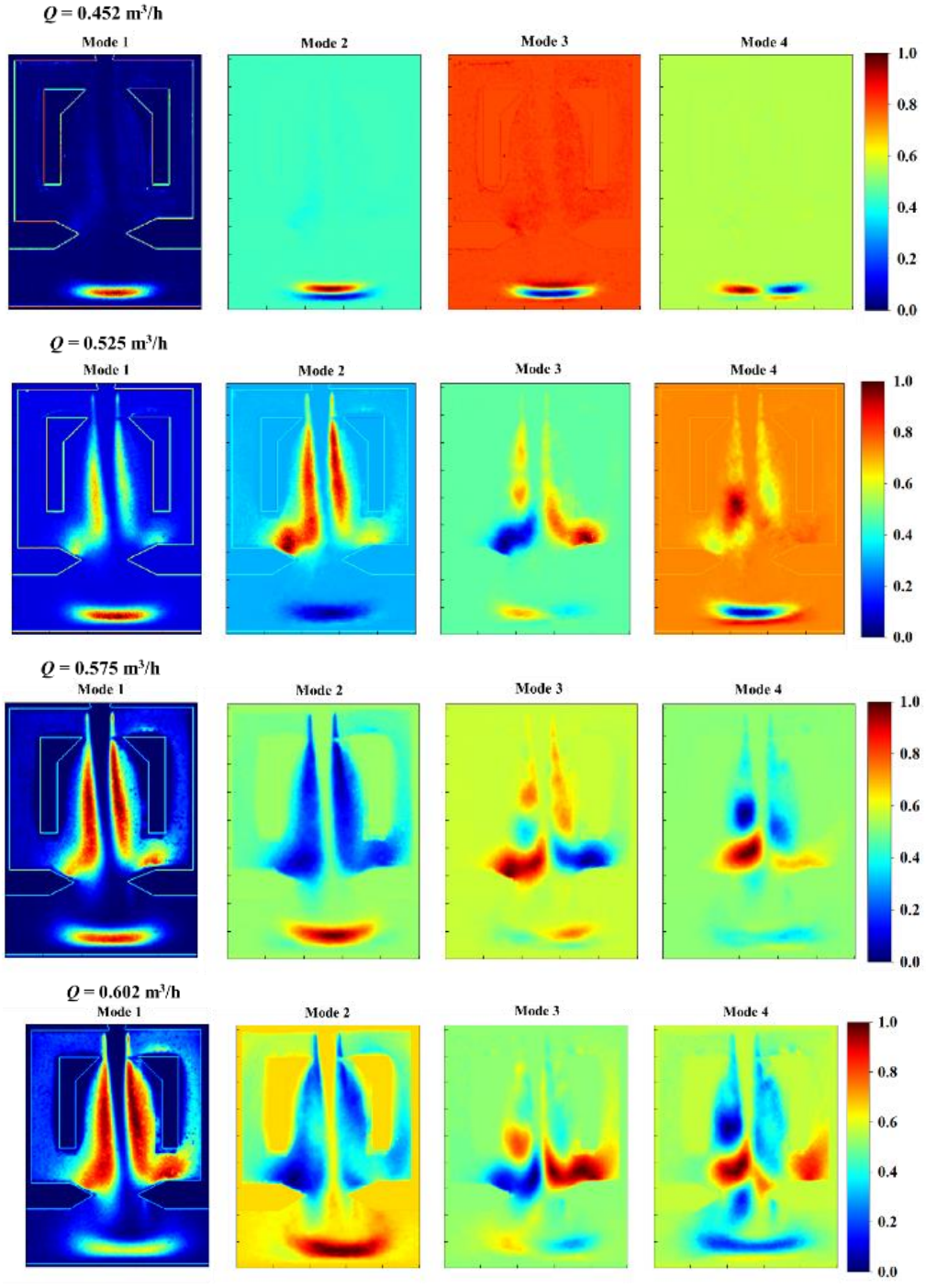

Fig. 12 Each mode contribution under different flow rates

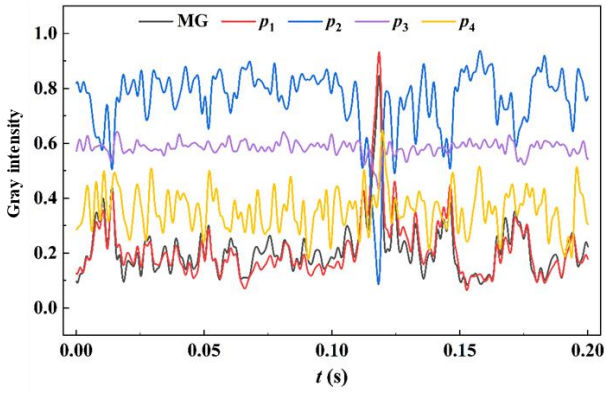

Fig. 13 Time domain diagram of the first four order mode coefficients and average gray values (Q = 0.525 m³/h)

cavitation cloud, which also shows a process of the continuous decomposition and detachment of the cavitation cloud with the development of the jet. Overall, the flow also affects the shape of the cavitation cloud. A higher flow rate may lead to a more irregular or elongated shape of the cavitation cloud. Additionally, the flow and deformation of the cavitation cloud in the flow field are more complicated due to the influence of shear forces.

In order to study the transient characteristics of the growth, development and collapse of the cavitation cloud in the cavitation jet, the reconstruction coefficient representing the time domain characteristics was analyzed. At the same time, the distribution of the reconstruction coefficient corresponding to each order mode function was studied. Figure 13 shows the change trend of the first four order modal coefficients and the average gray level of cavitation cloud over time with the inlet flow rate is Q = 0.525 m³/h. Comparing the first-order mode coefficient curve (p_1) with the average gray level curve (MG), it can be observed that the change trend of the two is consistent. The first-order mode coefficient can reflect the periodic pulsation of the main structure of the cavitation cloud, which is consistent with the overall change trend of the average gray level intensity of the cavitation cloud. This also indicates that the mode coefficient has a good representational ability in describing the gray level intensity of the image. Thus, the cavitation intensity can then be characterized.

4. CONCLUSION

In this paper, high - speed camera experiments are conducted to study the development characteristics of cavitation inside a fluidic oscillator under four different flow rates. The fluidic oscillator under study is a kind of positive feedback oscillator. The POD method is introduced and combined with the space-time distribution diagram of the cavitation cloud. The global distribution characteristics of the cavitation cloud are well revealed, and the flow field characteristics are analyzed. The basic idea of the POD method is to transform the data into a set of orthogonal basis functions namely eigenmodes or principal components through a singular value decomposition of the data matrix. These eigenmodes are listed in order of decreasing importance, with the previous modes containing the main patterns of change and energy of the data. Some significant conclusions regarding the cavitation development process in such a positive feedback fluidic oscillator are as follows:

(1) In the self-excited fluidic oscillator, cavitation mainly occurs in the region between the inner wall of the oscillator and the main jet, mainly reflected in the middle region between the two sides of the chamber and the two sides of the oscillator outlet, and the strength of cavitation under different flow rates is reflected in different cavitation regions.

(2) The oscillator inlet flow could affect the cavitation evolution rate. With the increase of flow rate, the evolution rate of the cavitation cloud would be faster. And then the cavitation cloud accelerates its expansion and deformation, forming a larger and more complex structure.

(3) The POD method is applied to perform mode decomposition of the cavitation flow field and extract the development characteristics of the cavitation cloud. The first-order mode has a high contribution rate to the flow field, and its shape is nearly identical with the average gray level image of cavitation cloud. Therefore, the first-order mode represents the aggregate average of the gray level field of the cavitation cloud, which can show the average flow distribution.

(4) The inlet flow affects the stability of the flow field structure, and the higher the inlet flow rate, the more unstable the cavitation flow field. Small-scale higher order modes can disclose the transient characteristics of cavitation cloud evolution in the cavitation jet, and low-order mode coefficients can characterize the cavitation intensity.

(5) This work mainly focuses on experimental research of the phenomenon of jet cavitation in oscillators. In future work, the combination of experimental and theoretical research can be strengthened. By combining large-scale experimental data with advanced numerical simulation techniques, a more complete and accurate model of jet cavitation flow can be established to conduct more in-depth simulation of cavitation phenomena under different working conditions. The structure and flow field parameters of the oscillator can be optimized to improve the stability and performance reliability of the equipment, and the mechanism of jet cavitation flow can be thoroughly studied, thereby improving the reliability and accuracy of research results.

ACKNOWLEDGEMENTS

This research is funded by the Qingdao Science and Technology for the Benefit of the People Demonstration Project (Grant No: 25-1-5-cspz-10-nsh), the Taishan Scholars Program and the Major innovation project in science, education and production of Qilu University of Technology (Shandong Academy of Sciences) (Grant No: 2023JBZ01).

CONFLICT OF INTEREST

The authors declare that they do not have any conflict of interest.

AUTHORS CONTRIBUTION

Zongrui Hao: Methodology, Data curation, Writing original draft, Funding acquisition. **Kailin Li:** Data curation, Validation, Software. **Ruihan Zhang**: Methodology, Software, Investigation. **Yue Wang:** Methodology, Investigation. **Gang Liu:** Writing – review & editing, Supervision, Funding acquisition.

REFERENCES

Al-Obaidi, A. R. (2019). Investigation of effect of pumprotational speed on performance and detection of cavitation within a centrifugal pump using vibration analysis. *Heliyon, 5*(6), e01910. https://doi.org/10.1016/j.heliyon.2019.e01910

Al-Obaidi, A., (2018). *Experimental and numerical investigations on the cavitation phenomenon in a centrifugal pump* [Doctoral dissertation, University of Huddersfield]. Huddersfield, UK.

Chatterjee, A., (2000). An introduction to the proper orthogonal decomposition. *Current Science*, *78*(7), 808-817. http://www.jstor.org/stable/24103957.

Chuah, L. F., Yusup, S., Abd Aziz, A. R., Bokhari, A., Klemeš, J. J., & Abdullah, M. Z. (2015). Intensification of biodiesel synthesis from waste cooking oil (Palm Olein) in a Hydrodynamic Cavitation Reactor: Effect of operating parameters on methyl ester conversion. *Chemical Engineering and Processing: Process Intensification*, *95*, 235-240. https://doi.org/10.1016/j.cep.2015.06.018

Danlos, A., Ravelet, F., Coutier-Delgosha, O., & Bakir, F. (2014). Cavitation regime detection through Proper Orthogonal Decomposition: Dynamics analysis of the sheet cavity on a grooved convergent–divergent nozzle. *International Journal of Heat and Fluid Flow*, *47*, 9-20. https://doi.org/10.1016/j.ijheatfluidflow.2014.02.001

Darandale, G. R., Jadhav, M. V., Warade, A. R., & Hakke, V. S. (2023). Hydrodynamic cavitation a novel approach in wastewater treatment: A review. *Materials Today: Proceedings*, *77*, 960-968. https://doi.org/10.1016/j.matpr.2022.12.075

Dhanke, P. B., & Wagh, S. M. (2020). Intensification of the degradation of Acid RED-18 using hydrodynamic cavitation. *Emerging Contaminants*, *6*, 20-32. https://doi.org/10.1016/j.emcon.2019.12.001

Dhanke, P., Wagh, S., & Kanse, N. (2018). Degradation of fish processing industry wastewater in hydro-cavitation reactor. *Materials Today: Proceedings*, *5*(2, Part 1), 3699-3703. https://doi.org/10.1016/j.matpr.2017.11.621

Dular, M., Khlifa, I., Fuzier, S., Adama Maiga, M., & Coutier-Delgosha, O. (2012). Scale effect on unsteady cloud cavitation. *Experiments in Fluids*, *53*(5), 1233-1250. https://doi.org/10.1007/s00348-012-1356-7

Feng, L. H., Wang, J. J., & Pan, C. (2011). Proper orthogonal decomposition analysis of vortex dynamics of a circular cylinder under synthetic jet control. *Physics of Fluids*, *23*(1). https://doi.org/10.1063/1.3540679

Ge, M., Manikkam, P., Ghossein, J., Kumar Subramanian, R., Coutier-Delgosha, O., & Zhang, G. (2022). Dynamic mode decomposition to classify cavitating flow regimes induced by thermodynamic effects. *Energy*, *254*, 124426. https://doi.org/10.1016/j.energy.2022.124426

Gohil, P. P., & Saini, R. P. (2015). Effect of temperature, suction head and flow velocity on cavitation in a Francis turbine of small hydro power plant. *Energy*, *93*, 613-624. https://doi.org/10.1016/j.energy.2015.09.042

Gore, M. M., Saharan, V. K., Pinjari, D. V., Chavan, P. V., & Pandit, A. B. (2014). Degradation of reactive orange 4 dye using hydrodynamic cavitation based hybrid techniques. *Ultrasonics Sonochemistry*, *21*(3), 1075-1082. https://doi.org/10.1016/j.ultsonch.2013.11.015

Hu, J., Yuan, M., Feng, G., Wang, X., & Li, D. (2023). Experimental investigation on the cavitation modulation mechanism in submerged self-sustained oscillating jets. *Ocean Engineering*, *274*, 114108. https://doi.org/10.1016/j.oceaneng.2023.114108

Huang, Y., Wu, Y., Huang, W., Yang, F., & Ren, X. E. (2013). Degradation of chitosan by hydrodynamic cavitation. *Polymer Degradation and Stability*, *98*(1), 37-43. https://doi.org/10.1016/j.polymdegradstab.2012.11.001

Hussain, L., & Khan, M. M. (2022). Recent progress in flow control and heat transfer enhancement of impinging sweeping jets using double feedback fluidic oscillators: A Review. *Journal of Heat Transfer*, *144*(12).doi: https://doi.org/10.1115/1.4055673

Joulaei, A., Nili-Ahmadabadi, M., & Yeong Ha, M. (2023). Numerical study of the effect of geometric scaling of a fluidic oscillator on the heat transfer and frequency of impinging sweeping jet. *Applied Thermal Engineering*, *221*, 119848. https://doi.org/10.1016/j.applthermaleng.2022.119848

Kim, S. H., & Kim, K. Y. (2019). Effects of installation conditions of fluidic oscillators on control of flow separation. *AIAA Journal*, *57*(12), 5208-5219. https://doi.org/10.2514/1.J058527

Liu, G., Bie, H., Hao, Z., Wang, Y., Ren, W., & Hua, Z. (2022). Characteristics of cavitation onset and development in a self-excited fluidic oscillator.

Ultrasonics Sonochemistry, *86*, 106018. https://doi.org/10.1016/j.ultsonch.2022.106018

Liu, X., Song, J., Li, B., He, J., Zhang, Y., Li, W., & Xie, F. (2021a). Experimental study on unsteady characteristics of the transient cavitation flow. *Flow Measurement and Instrumentation*, *80*, 102008. https://doi.org/10.1016/j.flowmeasinst.2021.102008

Liu, Y., Wu, Q., Huang, B., Zhang, H., Liang, W., & Wang, G. (2021b). Decomposition of unsteady sheet/cloud cavitation dynamics in fluid-structure interaction via POD and DMD methods. *International Journal of Multiphase Flow*, *142*, 103690. https://doi.org/10.1016/j.ijmultiphaseflow.2021.103690

Long, X., Zhang, J., Wang, J., Xu, M., Lyu, Q., & Ji, B. (2017). Experimental investigation of the global cavitation dynamic behavior in a venturi tube with special emphasis on the cavity length variation. *International Journal of Multiphase Flow*, *89*, 290-298. https://doi.org/10.1016/j.ijmultiphaseflow.2016.11.004

Madane, K. R., & Ranade, V. V., (2024). Solid-liquid flow in fluidic oscillator: Influence of solids on jet oscillations and residence time distribution. *Chemical Engineering Journal*, *485*, 149999. https://doi.org/10.1016/j.cej.2024.149999

Patil, P. N., Bote, S. D., & Gogate, P. R., (2014). Degradation of imidacloprid using combined advanced oxidation processes based on hydrodynamic cavitation. *Ultrasonics Sonochemistry*, *21*(5), 1770-1777. https://doi.org/10.1016/j.ultsonch.2014.02.024

Pawar, S. K., Mahulkar, A. V., Pandit, A. B., Roy, K., & Moholkar, V. S. (2017). Sonochemical effect induced by hydrodynamic cavitation: Comparison of venturi/orifice flow geometries. *AIChE Journal*, *63*(10), 4705-4716. https://doi.org/10.1002/aic.15812

Qiu, T., Wang, K., Lei, Y., Wu, C., Liu, Y., Chen, X., & Guo, P. (2018). Investigation on effects of back pressure on submerged jet flow from short cylindrical orifice filled with diesel fuel. *Energy*, *162*, 964-976. https://doi.org/10.1016/j.energy.2018.08.012

Seo, J. H., Zhu, C., & Mittal, R., (2018). Flow physics and frequency scaling of sweeping jet fluidic oscillators. *AIAA Journal*, *56*(6), 2208-2219. https://doi.org/10.2514/1.J056563

Simpson, A., & Ranade, V. V. (2019). Modeling hydrodynamic cavitation in venturi: influence of venturi configuration on inception and extent of cavitation. *AIChE Journal*, *65*(1), 421-433. https://doi.org/10.1002/aic.16411

Sonawat, A., Kim, S. J., Yang, H. M., Choi, Y. S., Kim, K. M., Lee, Y. K., & Kim, J. H. (2020). Positive displacement turbine - A novel solution to the pressure differential control valve failure problem and energy utilization. *Energy*, *190*, 116400. https://doi.org/10.1016/j.energy.2019.116400

Song, Y., Hou, R., Liu, Z., Liu, J., Zhang, W., & Zhang, L. (2022). Cavitation characteristics analysis of a novel rotor-radial groove hydrodynamic cavitation reactor. *Ultrasonics Sonochemistry*, *86*, 106028. https://doi.org/10.1016/j.ultsonch.2022.106028

Sun, Z., Li, D., Mao, Y., Feng, L., Zhang, Y., & Liu, C. (2022). Anti-cavitation optimal design and experimental research on tidal turbines based on improved inverse BEM. *Energy*, *239*, 122263. https://doi.org/10.1016/j.energy.2021.122263

Wang, B., Su, H., & Zhang, B. (2021). Hydrodynamic cavitation as a promising route for wastewater treatment – A review. *Chemical Engineering Journal*, *412*, 128685. https://doi.org/10.1016/j.cej.2021.128685

Wang, Z., Zhang, M., Kong, D., Huang, B., Wang, G., & Wang, C. (2018). The influence of ventilated cavitation on vortex shedding behind a bluff body. *Experimental Thermal and Fluid Science*, *98*, 181-194. https://doi.org/10.1016/j.expthermflusci.2018.05.029

Wei, Y., Zhang, H., Fan, L., Gu, Y., Leng, X., Deng, Y., & He, Z. (2022). Experimental study into the effects of stability between multiple injections on the internal flow and near field spray dynamics of a diesel nozzle. *Energy*, *248*, 123490. https://doi.org/10.1016/j.energy.2022.123490

Woszidlo, R., Ostermann, F., & Schmidt, H. J. (2019). Fundamental properties of fluidic oscillators for flow control applications. *AIAA Journal*, *57*(3), 978-992. https://doi.org/10.2514/1.J056775

Wu, Y., Yu, S., & Zuo, L. (2019). Large eddy simulation analysis of the heat transfer enhancement using self-oscillating fluidic oscillators. *International Journal of Heat and Mass Transfer*, *131*, 463-471. https://doi.org/10.1016/j.ijheatmasstransfer.2018.11.070

Xu, S., Long, X., Wang, J., Cheng, H., & Zhang, Z. (2022). Experiment on flow dynamics and cavitation structure in an axisymmetric venturi tube based on x-t diagrams and proper orthogonal decomposition. *Experimental Thermal and Fluid Science*, *136*, 110648. https://doi.org/10.1016/j.expthermflusci.2022.110648

Xu, S., Wang, J., Cheng, H., Ji, B., & Long, X. (2020). Experimental study of the cavitation noise and vibration induced by the choked flow in a Venturi reactor. *Ultrasonics Sonochemistry*, *67*, 105183. https://doi.org/10.1016/j.ultsonch.2020.105183

Zhang, Q., Gao, Y., Chu, M., Chen, P., Zhang, Q., & Wang, J. (2023). Enhanced energy conversion efficiency promoted by cavitation in gasoline direct injection. *Energy*, *265*, 126117. https://doi.org/10.1016/j.energy.2022.126117